NJC

Accepted Manuscript

This is an *Accepted Manuscript*, which has been through the Royal Society of Chemistry peer review process and has been accepted for publication.

Accepted Manuscripts are published online shortly after acceptance, before technical editing, formatting and proof reading. Using this free service, authors can make their results available to the community, in citable form, before we publish the edited article. We will replace this *Accepted Manuscript* with the edited and formatted *Advance Article* as soon as it is available.

You can find more information about *Accepted Manuscripts* in the Information for Authors.

Please note that technical editing may introduce minor changes to the text and/or graphics, which may alter content. The journal's standard Terms & Conditions and the Ethical guidelines still apply. In no event shall the Royal Society of Chemistry be held responsible for any errors or omissions in this *Accepted Manuscript* or any consequences arising from the use of any information it contains.

ROYAL SOCIETY OF CHEMISTRY

www.rsc.org/njc

New Journal of Chemistry

RSCPublishing

ARTICLE

High performance lithium sulfur battery with a cassava-derived carbon sheet as polysulfides inhibitor

Cite this: DOI: 10.1039/x0xx00000x

Furong Qin, Kai Zhang, Jing Fang*, Yanqing Lai, Qiang Li, Zhian Zhang, Jie Li

Received 00th January 2014,
Accepted 00th January 2014

DOI: 10.1039/x0xx00000x

www.rsc.org/

A biomass derived carbon material is obtained by simple carbonization of cassava and it is used to prepare carbon sheet as an interlayer for Li-S battery. The as-prepared carbon sheet possesses macroporous structure and high conductivity, which is in favor of electrolyte permeating and helps to accelerate the electrochemical kinetics. The cell with the as-prepared interlayer shows superior rate performance and cyclability. Even at ultrahigh rate (4 C, 1 C=1675 mAh g^{-1}_{sulfur}), a discharge capacity of 640 mA h g^{-1} is still retained for the cell. Meanwhile, the cell with the as-prepared interlayer exhibits superior reversible capacity of 811 mAh g^{-1} after 100 cycles at 0.5 C, and the discharge capacity retention is over 62%. The excellent electrochemical property probably is attributed to the high conductivity and macroporous structure of the as-prepared interlayer, which contribute to the accommodation of migrating polysulfides and accelerating the transfer of electron and ion, and consequently, enhance the electrochemical reactive activity of cathode as well as suppress the formation of Li_2S layer on the cathode.

1. Introduction

The lithium-sulfur battery is one of the most promising candidates for next generation energy storage devices, due to the low cost, non-toxicity and resource availability of sulfur. Its theoretical specific capacity and energy density reach as high as 1675 mAh g^{-1} and 2500 Wh kg^{-1}, respectively[1-3]. Nevertheless, there are many problems impeding its application such as low active material utilization, poor cycling stability, and poor rate performance[4, 5]. These problems are mainly attributed to two reasons: (a) the low electrical conductivity of sulfur and its reduction products (Li_2S or Li_2S_2)[6, 7]; (b) the dissolution and shuttle effect of the lithium polysulfides intermediate (Li_2S_n,$4\leq n\leq 8$) in organic liquid electrolytes during charging-discharging cycles[8-10].

To address these problems, it is necessary to enhance the conductivity of cathode and stabilize the active material within the cathode by using conductive materials (e.g., carbon-based materials[11, 12], conductive polymers[13, 14]). The most prevalent approaches to achieve this purpose are to use liquid-phase method and melting-diffusion method to confine sulfur in the conductive porous matrixes. The principle is that such porous conductive materials can provide diverse micro-/meso-/macro-pores to capture the active materials and accommodate sulfur. Following this principle, the most notable example is coming from the elegant work of Nazar et al.[15], which utilize highly ordered, mesoporous carbon to sequester sulfur and polysulfides. At a low discharge rate of 0.1 C, the capacities in excess of 800 mAh g^{-1} can be maintained in the pristine carbon material for 20 cycles. Another work of Archer[16] reports that the prepared porous hollow carbon@S composites can maintains a reversible capacity of 974 mAh g^{-1} after 100 cycles at 0.5 C. Recently, a new cell configuration, which contains a porous carbon interlayer between cathode and separator, has been put forward by Arumugam Manthiram[17-20] and his co-workers. For instance, relatively high specific area of carbon black[17] and multiwall carbon nanotubes[18] were used to fabricate interlayers for Li-S batteries and the electrochemical performance was remarkably enhanced. At the rate of 1 C, the reversible capacity can maintained over 900 mAh g^{-1}. Combining the sustainable concept, sucrose-coated eggshell membranes were also employed as carbon precursor to prepare carbon membrane[20]. When it was used as current collector and interlayer, the electrochemical performance of Li-S cells were greatly improved. It is considered that the interlayer can serve as a polysulfides barrier to limit polysulfides diffusion and localize the active material within the cathode side and buffer the volume change during cycling.

In this work, we try to use cassava, a high yield tropical crop whose thick roots can be used to produce starch, as carbon precursor to synthesize carbon material by simple carbonization process. This kind of cassava-carbon material (CCM) was applied to prepare cassava-carbon sheet (CCS) which was

New Journal of Chemistry Accepted Manuscript

placed between cathode and separator to use as polysulfides inhibitor for Li-S battery. Comparing to those method of preparing carbon interlayer in literatures, this approach has the advantages of low cost, large scale, activation free and easily to realization because of cassava's natural abundance and environment friendly property. It's worth noting that, although the cassava-carbon material used to make carbon interlayer has low specific surface area of 13.80 $m^2 g^{-1}$ and small pore volume of 0.015 $cm^3 g^{-1}$ at P/P_0 = 0.99, the cycle performance and the rate performance of the cell is also remarkably enhanced after insertion of the CCS. Investigation results show that the surface area of interlayer is not the key point that leads to high performance of Li-S cells. The porous structure and conductivity of interlayer may act as a more important role in improving cell performance.

2. Experimental procedures

2.1 Material preparation

The CCM was prepared by carbonizing the dry cassava under argon atmosphere from room temperature to 800 °C at a heating rate of 5 °C min^{-1} and the isothermal step lasts for 3 hours. The obtained monolithic cassava-carbon material was finely ground, and was mixed with polytetrafluoroethylene binder (PTFE, 5% suspension) at the 9:1 mass ratio, adding a small amount of isopropylalcohol in a mortar to form viscous slurry. Then the mixture was rolled into a membrane by a twin-roller and was dry in a vacuum oven at 60 °C. Finally it was punched into small disks (10 mm, diameter; ~0.2 mm, thickness; 7~10 mg, weight) to obtain the CCS.

2.2 Sample characterization

The morphology of the samples was investigated by scanning electron microscopy (JEOL, JSM-6360LV). The measurements of Brunauer–Emmett–Teller (BET) surface area and pore-size distributions were carried out with a volumetric sorption analyzer (ASAP 2020, Micromeritics) using physical adsorption/desorption of nitrogen gas at the liquid nitrogen temperature. Raman spectra of the dried sample were collected with LABRAM-HR 800 in the range of 2000~1000 cm^{-1} with He–Ne laser excitation at 532 nm. Thermogravimetric analysis (TGA, SDTQ600) was conducted to trace the carbonization process of the cassava under N_2 atmosphere at a heating rate of 10 °C min^{-1}. The conductivity of the CCS was measured by a standard four-probe method on a RTS-9 four-probe instrument at room temperature.

2.3 Electrochemical measurements

The electrodes were prepared by casting the homogeneous slurry which consisted of 60 wt.% sublimed sulfur (AR, 99.99%, Aladdin), 30wt.% acetyleneblack (Super P, Timcal) and 10 wt.% polyvinylidene fluoride (PVDF, Solef 6020) in N-methyl pyrrolidinone on the aluminum collector, and then dried at 60 °C overnight. Finally the cathode was cut into disks (10mm, diameter) and dried for 12 h in a vacuum oven at 60 °C. The sulfur content on each piece of cathode is ~1.6 mg cm^{-2}.

CR2025-type coin cells were assembled in a dry argon-filled glove box. The electrolyte used was 1 M bis(trifluoromethane) sulfonamidelithium salt (LiTFSI, 99.95%, Sigma Aldrich) in a mixed solvent of 1,3-dioxolane (DOL, 99.5%, Acros Organics) and 1,2-dimethoxyethane (DME, 99%Acros Organics) with a volume ratio of 1:1, including 0.1 M $LiNO_3$ as an electrolyte additive. Lithium metal was used as counter electrode and reference electrode and celgard-2400 was used as separator. The prepared CCS was placed between the cathode and the separator.

Cyclic voltammetry (CV) test and electrochemical impedance spectroscopy (EIS) measurements were conducted on Solartron 1470E electrochemical measurement system. The scanning rate of CV test is 0.2 mV S^{-1}, and the voltage range is 1.5~3.0 V. The impedance spectra were recorded at open-circuit potential (OCP) in the frequency range between 100 kHz and 10 mHz with a perturbation amplitude of 5 mV. Galvanostatic charge–discharge test were performed on a LAND CT2001A battery-testing instrument in the potential range of 1.8 ~ 3 V at 25 °C.

3. Results and Discussion

Fig. 1 shows the cell configuration for the Li-S battery with the CCS interlayer and the digital photograph of cassava raw materials. The carbon interlayer CCS was prepared by pyrolysis of cassava at 800 °C for 3 h, then mixed with PTFE binder at a 9:1 mass ratio, followed by roll-pressing and cutting into circular sheets. The obtained CCS is placed between the sulfur cathode and the separator, which is expected to improve the conductivity of the battery and capture the migrating polysulfides (Li_2S_x) from the cathode during electrochemical reactions.

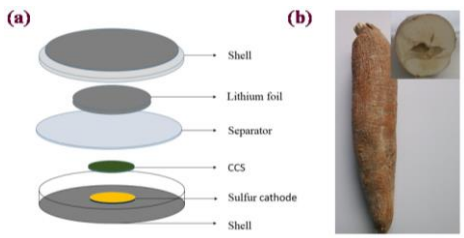

Fig. 1 (a) The schematic of cell configuration and (b) the photograph of raw cassava and its cross section (inset).

Fig. 2 shows the SEM results of the carbon powder derived from cassava and the surface of the as-prepared CCS. It is worth noting that the obtained CCM is still an intact monolith after the transformation of cassava to carbon. As shown in Fig. 2(a) and (b) the CCM retains interconnected porous honeycomb structure, which possesses a layered porous network with about 5~20 μm of large pore diameter and very thin pore wall. After being made into sheet, the porous structure of CCM still be maintained in CCS (seen in Fig. 2(c) and (d)), only the surface become smooth.

New Journal of Chemistry Accepted Manuscript

 This journal is © The Royal Society of Chemistry 2014

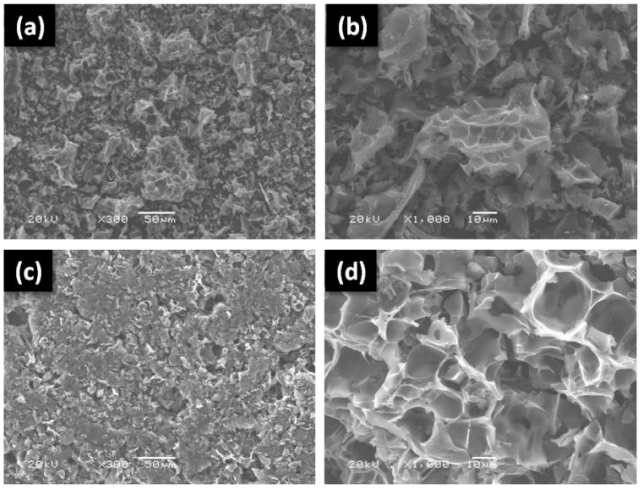

Fig. 2 SEM images of (a, b) the powder of cassava-carbon material (CCM) and (c, d) the surface of cassava-carbon sheets (CCS)

N_2 adsorption/desorption measurement was employed to character the textural properties of CCM. Fig. 3 depicts the isotherm plot and pore size distribution derived from desorption branch of CCM. The result shows that the CCM has very low BET surface area of 13.80 m^2 g^{-1} (t-plot micropore area is 6.37 m^2 g^{-1} and t-plot external surface area is 7.43 m^2 g^{-1}) and a pore volume of 0.015 cm^3 g^{-1} (single point at P/P_0=0.99) and the average pore diameter is less than 4.4 nm (by BET). The data is much smaller than that of microporous carbon paper, MWCNTs, and carbonized eggshell membrane mentioned in literature 17, 18 and 20. The N_2 adsorption-desorption measurement combined SEM results indicate that the CCM is mainly composed of little amount of micropores and mesopores and certain amount of macropores. The conductivity of the CCS measured by four-probe method is 13.16 S cm^{-1}. These hierarchical porous architecture and good conductivity may help to absorb the liquid electrolyte, accommodate polysulfides, transport electron and enhance the cathode conductivity[18, 21, 22].

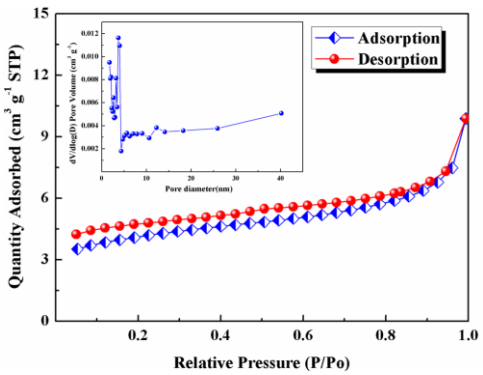

Fig.3 N_2 adsorption/desorption isotherm and (inset) BJH pore size distribution of CCM.

Fig. 4(a) shows the TG and DTA curves of cassava under N_2 atmosphere. As can be seen from Fig. 4(a), there are two weight-loss stages. The first stage is in the range from 30 °C to 130 °C. Along with this stage, a small endothermic peak was found, which indicate the evaporation of water. The second stage is in the range from 270 °C to 340 °C in which nearly 80 % of the weight was lost, and it should be related to the degradation of cellulose and the loss of H, O atom in the cassava. From the TGA curve it can be learn that the conversion rate of cassava to carbon is about 20 wt. %. Fig. 4(b) presents the Raman spectrum of the carbonized cassava. As can be seen from Fig. 4(b), it possesses two main peaks at 1323 and 1588 cm^{-1}, which are associated with the disordered carbon and graphitized carbon, respectively. This result indicates the partly graphitization of cassava in the pyrolysis process at 800 °C, which is beneficial for promoting the conductivity of CCS.

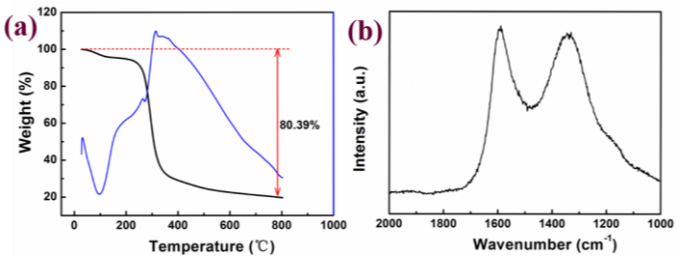

Fig. 4 (a) TGA curves of the cassava material and (b) Raman spectra of the CCM

Cyclic voltammogram (CV) curves of the Li–S batteries without and with CCS interlayer are presented in Fig. 5(a) and (b). In the cathodic scan, all samples present two remarkable reduction peaks at about 2.04 V and 2.28 V which correspond to the two discharge plateaus in Fig. 5(c) or (d). The peak at ~2.28 V is related to the conversion of elemental sulfur to soluble lithium polysulfides (Li_2S_x,4≤x≤8), and the reduction peak at ~2.04 V is related to the reduction of lithium polysulfides to insoluble Li_2S_2 and Li_2S[23, 24]. In the subsequent anodic scan, only one broad oxidation peak is observed in the potential range of 2.45 -2.55 V, which corresponds to the conversion of Li_2S_2 or Li_2S into soluble lithium polysulfides and elemental sulfur[25-27]. The slight over-potential in the initial cathodic and anodic sweep in cell with CCS interlayer is attributed to the polarization caused by the phase transition from the conversion–dissolution-diffusion process of the sulfur and polysulfides[17]. Compared to the cell without interlayer, the cell with CCS interlayer seem to show more polarization in the first cycle, it may also due to the interlayer not be well infiltrated by electrolyte at early stage. But after the first cycle, the over-potential of the first cathodic or anodic peak disappears, possibly due to the rearrangement of the migrating active material to electrochemically favorable positions[17]. Afterwards, the anodic and cathodic peaks of CV curves for the cell with CCS are well overlapped, suggesting less polarization and high reversibility in the following cycles.

New Journal of Chemistry Accepted Manuscript

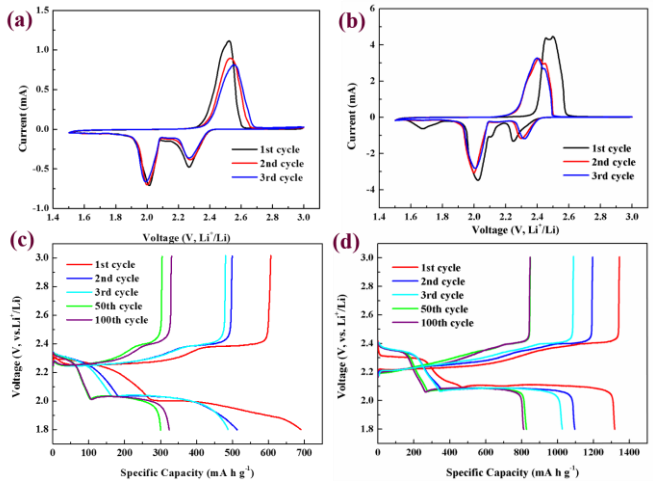

Fig. 5 CV curves of the Li–S batteries (a) without and (b) with CCS interlayer at 0.2 mV s^{-1}; Discharge-charge profiles of the Li–S batteries (c) without and (d) with CCS interlayer at 0.5 C.

Fig. 5(c) and (d) shows the discharge/charge voltage profiles of the cell without and with CCS interlayer at 0.5 C (1 C= 1675 mA g^{-1}_{sulfur}) respectively, and all the capacity are calculated by the weight of sulfur. Two discharge and one charge potential plateaus can be apparently observed from both figures, which are corresponding to the two steps reaction of S during the discharge process as demonstrated in CV measurements. As shown in Fig. 5(d), the cell with CCS interlayer shows an initial specific discharge capacity of 1318 mA h g^{-1} and maintains a reversible capacity of 811 mA h g^{-1} after 100 cycles at a rate of 0.5 C, which indicate that the CCS interlayer is quite effective in maintaining high utilization of the active sulfur and suppressing the dissolution of polysulfides into the electrolyte during the discharge/charge process. The 50th and the 100th charge and discharge profiles are well overlapped, which indicates the high cyclability of the lithium sulfur battery with CCS interlayer.

The cycle performance of the cells with and without CCS interlayer at a rate of 0.5 C between 3.0 V and 1.8 V is displayed in Fig. 6(a). It can be seen that the CCS interlayer can greatly enhance the capacity of the cell. After 100 cycles at 0.5 C rate, the reversibly capacity of the sample with CCS is 811 mAh g^{-1} (based on the mass of sulfur) with 62 % capacity retention. The superior cycle performance is similar to that of cells with other interlayers reported before[17, 18, 20], while the sample without interlayer retains only 324 mAh g^{-1} discharge capacity after 100 cycles. The remarkably improved cyclic performance of the cell with CCS interlayer may be attributed to the macroporous interlayer frame work, providing electronic conductive network to suppress soluble long-chain polysulfides diffusing to the anode and enhance the active material utilization[28].

Fig. 6(b) displays the rate performance of Li–S cell with and without the insertion of CCS interlayer. It is clearly seen that the cell with CCS interlayer exhibits excellence performance at different current densities. During the first 6 cycles, the discharge capacity faded gradually at 0.1 C rate and remained the capacity of 1012 mAh g^{-1}. At higher rate of 0.2 C and 0.5 C, the capacity of 971 mAh g^{-1} and 888 mAh g^{-1} can be delivered respectively. Then, further increasing the charge/discharge current to 1 and 2 C, a reversible capacity of 854 mAh g^{-1} (60% of the initial capacity) and 834 mAh g^{-1} (58% of the initial capacity) is reached, respectively. It is more remarkable that the cell can even delivered a capacity of 640 mAh g^{-1} at ultrahigh rate of 4 C. All these results demonstrate the prominent rate performance of the cell with CCS interlayer. When the charge/discharge rate is abruptly set back to 0.5 C after being continuously cycled at high rates for 20 times, a reversible capacity of 909 mAh g^{-1} can still be restored, suggesting excellent redox stability of the cell with CCS interlayer. By contrast, the cell without CCS interlayer shows fast capacity fading at the same increasing the charge–discharge rate. The excellent rate performance of the cell with CCS may be attributed to the good conductivity of cassava-carbon material, which can increase the electronic conductivity of the cathode. Furthermore, the porous cassava-carbon material can act as a secondary current collector in which the sulfur species are distributed and tightly trapped, as well as a reservoir of liquid electrolyte in which the transfer of lithium ion to active material can be accelerated[29, 30].

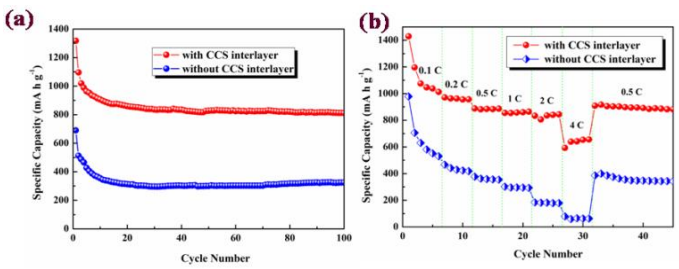

Fig. 6 (a) Cycling performance of the Li–S batteries with and without CCS interlayer at 0.5 C. (b) Rate performance of the Li–S batteries with and without CCS interlayer.

The Nyquist plots of the Li-S cells (full charge) without and with the CCS interlayer at its OCP before the first discharge and after the 100th charge are shown in Fig. 7(a) and (b), and the insets are the used equivalent circuits for fitting. It can be seen that the Nyquist plots of both cells before 1st cycle are composed of a semicircle at high-to-medium frequency and an inclined line at low frequency region. The high-frequency intercept on the real axis represents the ohmic resistance (R_o) of the cell, including the electrolyte and electrode resistances. The semicircle at high frequency to medium is attributed to the interface charge-transfer resistance (R_{ct}), and the inclined line at the low-frequency region corresponds to Warburg impedance (W_o)[19]. Before cycle, the impedance semi-circle after the insertion of CSS interlayer does not change apparently and the R_{ct} of both cells is ~38 Ω, which demonstrating the same charge transfer of both cells. After 100th cycles, the impedance responses of two cells have changed that two obvious semicircles appear, as shown in Fig. 7(a) and (b).The emerged new semicircle at higher frequency region is related to the solid-electrolyte interface (SEI) film formed during the charge-

New Journal of Chemistry Accepted Manuscript

This journal is © The Royal Society of Chemistry 2014

discharge process[31, 32]. The fitted R_o, R_s, and R_{ct} values of two cells according to the equivalent circuit are shown in Table 1.

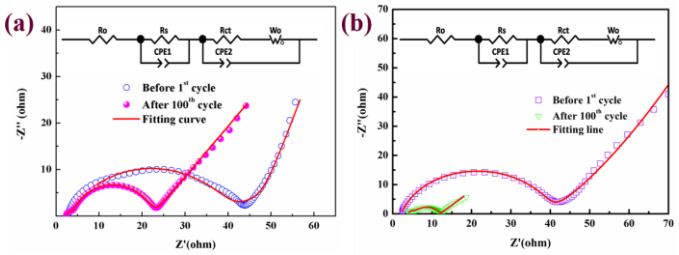

Fig. 7 The EIS spectra of the cells (full charge) (a) without and (b) with CCS interlayer. Insets are the used equivalent circuit.

Table 1 Fitted R_o, R_s, and R_{ct} values of the as-fabricated samples at the OCP state before cycle and after 100th cycle at 0.5 C

	Impedance values	R_o (Ω)	R_s (Ω)	R_{ct} (Ω)
Without CCS	Before 1st cycle	2.1	-	38.7
	After 100th cycle	2.4	1.1	19.0
With CCS	Before 1st cycle	2.0	-	38.0
	After 100th cycle	4.0	1.0	7.0

After 100 cycles, the R_o value of the cell without CCS interlayer shows slight increase. However, the R_o value of the one with CCS interlayer increase remarkably, which maybe attributes to more elemental sulfur regenerating after charging since the EIS measurements were conducted at full-charge state. That is to say, the utilization of sulfur is much higher after inserting an interlayer. The semicircle at high frequency is related to the resistance and capacitance (a parallel connection of R_s and CPE_1) of solid-state interface layers on the surfaces of the electrodes, which reflects the resistance over lithium ion diffusion through the contacting interface and Li_2S/Li_2S_2 solid film[33]. The semicircle at medium frequency is related to the charge-transfer resistance against the interfacial electrochemical reaction involved in charge transfer and its related double layer capacitance (parallel connection of R_{ct} and CPE_2)[34]. After cycles, the R_s of both cells is about 1 Ω, meanwhile the charge-transfer resistance R_{ct} decreased remarkably, which indicates SEI film was formed and the increased active sites for interfacial electrochemical reaction[35]. By contrast, the R_{ct} of the cell with CCS interlayer decreased more apparently (it decreased to ~7 Ω, but that of without interlayer only decreased to ~19 Ω), suggesting the CSS interlayer can help to decrease charge transfer resistance in cycle process. The EIS results further reveal that the CCS interlayer may increase the reactive contact area and improve the electrochemical environment of reaction with continuous immersion of the electrolyte in the cell. It also explains why the cell with CCS interlayer possesses good electrochemical kinetics and excellent performance.

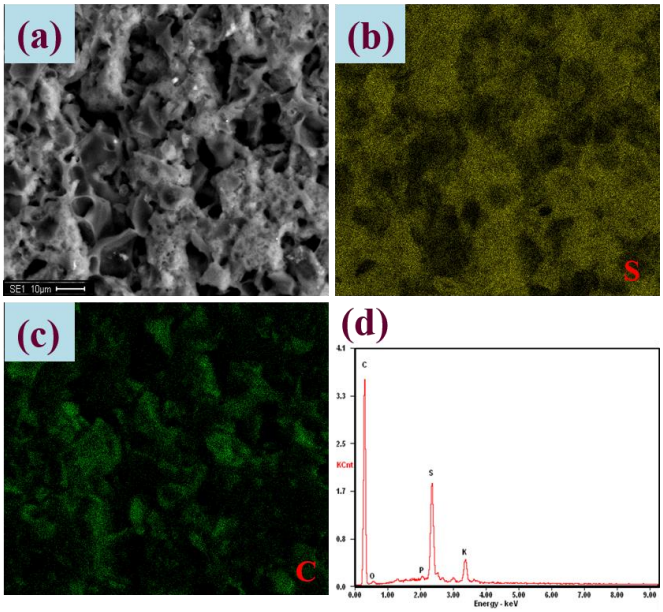

Fig. 8 (a) the SEM image, corresponding EDS elemental mapping of (b) sulfur and (c) carbon, and (d) the EDS spectrum of CCS interlayer after 100 cycles at 0.5 C rate.

To get further insight into the excellent electrochemical performance of the Li-S cell with the CCS interlayer, the cell after cycled was disassembled and the morphology of the CCS interlayer after 100 cycles is characterized. As shown in Fig. 2(c) and (d), before cycle, the CCS interlayer shows interconnected structure with macropores, which enables the easy infiltration of the electrolyte into the interlayer. Therefore, good rate capability can be achieved for the cell with CCS interlayer. After long-time charge/discharge cycles, from the Fig. 8 (a), it can be seen that the CCS interlayer still maintains a stable porous structure and no obvious damage. From the morphology of CCS, it can be observed that some pores were blocked by precipitate. The results of EDS element distribution from Fig. 8(b) and Fig. 8(c) shows that the precipitate blocked in the pores mainly contains elemental S, implying the entry and aggregation of polysulfides in the pores of interlayer, which further confirms the capturing and accommodating act of the porous CCS interlayer for active sulfur. Furthermore, this interconnected "honeycomb-like" CCS interlayer can act as a continuous conductive 3D network, which could provide efficient accessibility of active material to the electrolyte and rapid electron transfer, and consequently, making the capture of sulfur can be reutilized. The SEM and EDS results demonstrate the interconnected porous structure of CCS interlayer are helpful to accommodating sulfur species, and inhibiting polysulfides dissolving and migrating. It also explains that why the cell with CCS interlayer exhibits good cycle stability and rate capability although the cassava-carbon material (CCM) used to make CCS has low specific surface area.

4. Conclusions

In this paper, a porous biomass-derived carbon materials, synthesized by simple carbonizing cassava, is used to prepare

New Journal of Chemistry Accepted Manuscript

interlayer for Li-S battery, which significantly enhance the electrochemical performance of the cell. The results show that the cell with the CCS interlayer exhibits excellent cycle stability and superior rate capability, even though the surface area of cassava-derived carbon material which employed to make CCS interlayer is very small. Discharge capacities of 811 mAh g^{-1} after 100 cycles at 0.5 C and 640 mAh g^{-1} at 4 C are achieved. This results show that the surface area of the interlayer is not the key roll to restrict the dissolution of polysulfides. The improvement probably was due to the interconnected macroporous structure of CCS interlayer, providing a conductive framework to accommodate and reutilize polysulfides and confine them in the cathode side, at the same time increasing the efficient accessibility of active material to the electrolyte and charge, thus enhancing the transfer of ion and electron. This biomass derived carbon would be a promising material for the preparation of interlayer for Li-S batteries and the simple synthetic method is expected to be practically applicable for high-performance Li-S batteries as the next generation energy storage systems.

Acknowledgements

We gratefully acknowledge the financial support of National Natural Science Foundation of China (51222403), the Excellent Youth Foundation (13JJ1003) and Natural Science Foundation of Hunan Province (14JJ2001), and Fundamental Research Funds for the Central Universities (2012QNZT023) of China. We also thank the support of the Engineering Research Centre of Advanced Battery Materials, the Ministry of Education, China.

Notes and references

*School of Metallurgy and Environment, Central South University, Changsha 410083, China.
E-mail: fangjing526@csu.edu.cn.

1. P. G. Bruce, S. A. Freunberger, L. J. Hardwick and J. M. Tarascon, *Nat. Mater.*, 2012, **11**, 19.
2. B. Scrosati, J. Hassoun and Y. K. Sun, *Energy Environ. Sci.*, 2011, **4**, 3287.
3. X. Ji and L. F. Nazar, *J. Mater. Chem.*, 2010, **20**, 9821.
4. M. K. Song, E. J. Cairns and Y. Zhang, *Nanoscale*, 2013, **5**, 2186.
5. Y. Yang, G. Zheng and Y. Cui, *Chem. Soc. Rev.*, 2013, **42**, 3018.
6. S. E. Cheon, K. S. Ko, J. H. Cho, S. W. Kim, E. Y. Chin and H. T. Kim, *J. Electrochem. Soc.*, 2003, **150**, A796.
7. S. E. Cheon, K. S. Ko, J. H. Cho, S. W. Kim, E. Y. Chin and H. T. Kim, *J. Electrochem. Soc.*, 2003, **150**, A800.
8. Y. Diao, K. Xie, S. Xiong and X. Hong, *J. Power Sources*, 2013, **235**, 181.
9. Y. V. Mikhaylik and J. R. Akridge, *J. Electrochem. Soc.*, 2004, **151**, A1969.
10. S. S. Zhang, *J. Power Sources*, 2013, **231**, 153.
11. K. Zhang, J. Li, Q. Li, J. Fang, Z. Zhang, Y. Lai and Y. Tian, *J. Solid State Electrochem.*, 2013, **17**, 3169.
12. Y. Qu, Z. Zhang, X. Wang, Y. Lai, Y. Liu and J. Li, *J. Mater. Chem. A*, 2013, **1**, 14306.
13. X. Zhao, J. K. Kim, H. J. Ahn, K. K. Cho and J. H. Ahn, *Electrochim. Acta*, 2013, **109**, 145.
14. W. Zhou, Y. Yu, H. Chen, F. J. DiSalvo and H. D. Abruña, *J. Am. Chem. Soc.*, 2013, **135**, 16736.
15. X. Ji, K. T. Lee and L. F. Nazar, *Nat. Mater.*, 2009, **8**, 500.
16. N. Jayaprakash, J. Shen, S. S. Moganty, A. Corona and L. A. Archer, *Angew. Chem. Int. Ed. Engl.*, 2011, **50**, 5904.
17. Y. S. Su and A. Manthiram, *Nat. Commun.*, 2012, **3**, 1166.
18. Y. S. Su and A. Manthiram, *Chem. Commun.*, 2012, **48**, 8817.
19. C. Zu, Y. Su, Y. Fu and A. Manthiram, *Phys. Chem. Chem. Phys.*, 2013, **15**, 2291.
20. S. H. Chung and A. Manthiram, *Adv. Mater.*, 2014, **26**, 1360.
21. K. Zhang, Q. Li, L. Zhang, J. Fang, J. Li, F. Qin, Z. Zhang and Y. Lai, *Mater. Lett.*, 2014, **121**, 198.
22. Y. Sudaryanto, S. B. Hartono, W. Irawaty, H. Hindarso and S. Ismadji, *Bioresour. Technol.*, 2006, **97**, 734.
23. Y. Jung and S. Kim, *Electrochem. Commun.*, 2007, **9**, 249.
24. Y. Li, H. Zhan, S. Liu, K. Huang and Y. Zhou, *J. Power Sources*, 2010, **195**, 2945.
25. X. Tao, X. Chen, Y. Xia, H. Huang, Y. Gan, R. Wu, F. Chen and W. zhang, *J. Mater. Chem. A*, 2013, **1**, 3295.
26. J. Guo, Z. Yang, Y. Yu, H. D. Abruna and L. A. Archer, *J. Am. Chem. Soc.*, 2013, **135**, 763.
27. G. Zhou, L. C. Yin, D. W. Wang, L. Li, S. Pei, I. R. Gentle, F. Li and H. M. Cheng, *ACS Nano*, 2013, **7**, 5367.
28. K. Zhang, F. Qin, J. Fang, Q. Li, M. Jia, Y. Lai, Z. Zhang and J. Li, *J. Solid State Electrochem.*, 2013, **18**, 1025.
29. S. H. Chung and A. Manthiram, *J. Mater. Chem. A*, 2013, **1**, 9590.
30. S. H. Chung and A. Manthiram, *Electrochim. Acta*, 2013, **107**, 569.
31. J. Xie, J. Yang, X. Zhou, Y. Zou, J. Tang, S. Wang and F. Chen, *J. Power Sources*, 2014, **253**, 55.
32. X. Zhou, J. Xie, J. Yang, Y. Zou, J. Tang, S. Wang, L. Ma and Q. Liao, *J. Power Sources*, 2013, **243**, 993.
33. Z. Deng, Z. Zhang, Y. Lai, J. Liu, J. Li and Y. Liu, *J. Electrochem. Soc.*, 2013, **160**, A553.
34. V. S. Kolosnitsyn, E. V. Kuzmina, E. V. Karaseva and S. E. Mochalov, *J. Power Sources*, 2011, **196**, 1478.
35. Q. Li, Z. Zhang, K. Zhang, J. Fang and Y. Q. Lai, *J. Power Sources*, 2014, **256**, 137.

New Journal of Chemistry Accepted Manuscript

 This journal is © The Royal Society of Chemistry 2014